Biogeosciences Discuss., 11, 4335–4358, 2014
www.biogeosciences-discuss.net/11/4335/2014/
doi:10.5194/bgd-11-4335-2014

Biogeosciences Discussions
Open Access

The sensitivity of primary productivity to intra-seasonal mixed layer variability in the sub-Antarctic Zone of the Atlantic Ocean

W. R. Joubert[1,2], **S. Swart**[1], **A. Tagliabue**[1,2,3], **S. J. Thomalla**[1], **and P. M. S. Monteiro**[1,2]

[1]Southern Ocean Carbon and Climate Observatory, Council for Scientific and Industrial Research, Jan Cilliers Street, Stellenbosch, 7600, South Africa
[2]Department of Oceanography, University of Cape Town, Rondebosch, 7700, South Africa
[3]School of Environmental Sciences, University of Liverpool, Liverpool L69 3GP, UK

Received: 3 February 2014 – Accepted: 24 February 2014 – Published: 18 March 2014

Correspondence to: W. R. Joubert (wjoubert@csir.co.za)

Published by Copernicus Publications on behalf of the European Geosciences Union.

Abstract

The seasonal cycle of primary productivity is impacted by seasonal and intra-seasonal dynamics of the mixed layer through the changing balance between mixing and buoyancy forcing, which regulates nutrient supply and light availability. Of particular recent interest is the role of synoptic scale events in supplying nutrients, particularly iron, to the euphotic zone in the Sub Antarctic Zone (SAZ), where phytoplankton blooms occur throughout summer. In this study, we present high resolution measurements of net community production (NCP) constrained by $\Delta O_2/Ar$ ratios, and mixed layer depth (MLD) in the Atlantic SAZ. We found a non-linear relationship between NCP and MLD, with the highest and most variable NCP observed in shallow MLDs (< 45 m). We propose that NCP variability in the SAZ may be driven by alternating states of synoptic-scale deepening of the mixed layer, leading to the entrainment of iron (dFe), followed by restratification, allowing rapid growth in an iron replete, high light environment. Synoptic iron fluxes into the euphotic zone based on water column dFe profiles and high resolution glider MLD data, reveal a potentially significant contribution of "new iron" which could sustain NCP throughout summer. Future process studies will help elaborate these findings further.

1 Introduction

Two of the principal drivers of the High Nutrient Low Chlorophyll (HNLC) characteristics (Chisholm and Morel, 1991) of the Southern Ocean are limitation by light (Mitchell et al., 1991) and iron (Martin et al., 1991; Boyd et al., 2007). The impact of these limiting factors on primary production varies over the growing season (Boyd, 2002). For instance during winter, increased light limitation is observed due to deep mixed layers caused by high rates of convective overturning (DeBoyer-Montégut, 2004). However, deep winter mixing also restores the Fe supply to the euphotic zone and relieves Fe limitation for the onset of the spring bloom (Boyd, 2002; Thomalla et al., 2011; Tagli-

BGD
11, 4335–4358, 2014

abue et al., 2014). Throughout spring and summer, the iron supplied to the euphotic zone from the pulse of winter convective overturning is depleted in the euphotic zone (Boyd, 2002; Tagliabue et al., 2014). The complex role of these multiple driving factors is emphasised by the large-scale spatial variability of chlorophyll *a* (chl *a*), which highlight regional differences in phytoplankton biomass attributed to variability in seasonal physics and biogeochemical dynamics (Arrigo et al., 2008; Moore and Abbott, 2000). Recent work using satellite data has proposed that phytoplankton variability during spring and summer in the Southern Ocean can be influenced by intra-seasonal adjustments of the mixed layer physics that modulate light and nutrient limitation (Fauchereau et al., 2011; Thomalla et al., 2011).

In the Southern Ocean, the limiting nutrient iron can be supplied vertically into the euphotic zone by once off wintertime convective overturning (entrainment), and year-round diapycnal diffusion, as well as Ekman upwelling (Boyd and Ellwood, 2012; Tagliabue et al., 2014). Determining vertical supply rates of iron requires knowledge of the water column iron distribution and the depth of the ferricline plays an important role. Using dissolved iron (dFe) measurements, Tagliabue et al. (2014) reported the depth of the ferricline in the Sub-Antarctic Zone (SAZ) to be between 200–500 m, which results in weak diapycnal diffusive fluxes (up to 15 nmol Fe $m^{-2} d^{-1}$) in the region. In the Drake Passage, Frants et al. (2013) reported relatively high in situ estimates of diapycnal diffusion up to 64 ± 2 nmolFe $m^{-2} d^{-1}$ assuming vertical diffusivity (K) of 1×10^{-4} $m^2 s^{-1}$. Based on the dFe gradient with depth and monthly mixed layer changes, the authors also calculated entrainment due to mixed layer deepening of 5–25 nmol Fe $m^{-2} d^{-1}$. Lower diffusive fluxes of 15 nmol Fe $m^{-2} d^{-1}$ were observed in the SAZ south of Tazmania, calculated using vertical diffusivity from in situ microturbulence observations (Boyd et al., 2005). All these estimates exclude synoptic or sub seasonal scale processes in their assessments of iron input.

A number of physical processes, at a range of sub-seasonal scales, are known to modulate MLD variability and primary production (Lévy et al., 2012). For example, in regions of high dynamic variability, mesoscale (10–100 km) and submesoscale dynamics

BGD
11, 4335–4358, 2014

(1–10 km), are known to stimulate ocean productivity at similar scales through the vertical transport (advection and diffusion) of subsurface nutrients in oligotrophic ocean regions (Lathuiliere et al., 2011; Lévy et al., 2009; McGillicuddy et al., 2007; Oschlies and Garcon, 1998). Similarly, under low light conditions, enhanced rates of re-stratification associated with lateral advection from eddy and frontal instabilities (i.e., Taylor and Ferrari, 2011; Mahadevan et al., 2012) reduce the depth of the mixed layer, thereby increasing the exposure of phytoplankton to light in the euphotic zone (Sverdrup, 1953) favouring production. These findings indicate strong links between fine temporal (seasonal to sub-seasonal) and spatial (mesoscale to sub-mesoscale) scales of mixed layer dynamics and their influence on primary production.

Net community production (NCP) reflects the balance between net primary production and heterotrophic respiration integrated through the mixed layer (Siegel et al., 2002). NCP is equivalent to new production, and approximates organic carbon export from the surface ocean (Falkowski et al., 2003). In order for net autotrophy to occur, in other words a positive NCP, the mixed layer is required to be shallower than a critical depth where water column integrated growth and loss rates are equal (Sverdrup, 1953). In iron-limited waters an additional consideration is that process studies (e.g., Boyd et al., 2005) have demonstrated that productivity can be sustained by recycled iron, highlighting the importance of the so-called "ferrous wheel" (Strzepek et al., 2005). When viewed as "fe-ratios" (uptake of new iron/uptake of total iron) new iron has been shown to account as little as 10 % or as much as 50 % (from low to high iron waters) of the overall iron demand (Boyd et al., 2005; Bowie et al., 2009; Sarthou et al., 2008). Nevertheless, NCP has been shown to be consistently low when mixed layers are deep, regardless of iron sufficiency (Cassar et al., 2011). What remains uncertain is the response of NCP to intraseasonal variability in the MLD, which may influence the inputs of iron into the euphotic zone.

In this study, we present high resolution NCP estimates based on continuous shipboard measurements of $\Delta O_2/Ar$ ratios (and NCP) (Cassar et al., 2009) collected from several repeat transects in the Atlantic SAZ during austral summer. We investigate the

BGD
11, 4335–4358, 2014

relationship between NCP and co-located MLD across the Sub-Tropical (STZ), SAZ and the Polar Frontal Zone (PFZ). We highlight the role of intraseasonal mechanisms that drive the variability of NCP in the context of mixed layer dynamics and explore a link between summer entrainment of dFe and sustained summer blooms (Swart et al., 2014).

2 Data and methods

Five crossings in the Atlantic sector of the Southern Ocean were conducted between 2008 and 2010 (Fig. 1) along the GoodHope monitoring line (Swart et al., 2008; Arhan et al., 2011). The transects crossed major hydrographic fronts of the Southern Ocean, namely the Subtropical Front (STF, $\sim 40^{\circ}$ S), the Sub-Antarctic Front (SAF, $\sim 44^{\circ}$ S), and the Polar Front (PF, $\sim 50^{\circ}$ S) (Fig. 1). The SAZ lies between the STF and the SAF, while the PFZ is delimited by the SAF to the north and the PF to the south.

Continuous underway measurements of O_2/Ar ratios were made on the ship's seawater supply using Equilibrator Inlet Mass Spectrometry (Cassar et al., 2009). NCP was determined from biological oxygen supersaturation ($\Delta O_2/Ar$) (Craig and Hayward, 1987). Biological oxygen saturation is defined as:

$$\Delta O_2/Ar = [(O_2/Ar)_{sample}/(O_2/Ar)_{sat}] - 1 \quad (1)$$

$(O_2/Ar)_{sample}$ and $(O_2/Ar)_{sat}$ is the seawater sample and saturation ratio, respectively. A positive $\Delta O_2/Ar$ value indicates net autotrophic conditions and reflects the combined oxygen balance of the entire community. Assuming no vertical or lateral exchanges, NCP (in units of mmol m^{-2} d^{-1}) is the biological oxygen flux between the surface ocean and overlying atmosphere. NCP is estimated by

$$NCP = k_w \cdot (\Delta O_2/Ar) \cdot (O_2)_{sat} \cdot \rho \quad (2)$$

where k_w is the weighted gas transfer velocity for O_2 (m d^{-1}), $(O_2)_{sat}$ is the saturation concentration of oxygen in the mixed layer (mmol kg^{-1}) and ρ is the density of seawater

BGD
11, 4335–4358, 2014

($kg\,m^{-3}$) (Cassar et al., 2009). The gas transfer velocity for oxygen was estimated using windspeed from the NCEP/NCAR reanalysis data product and the parameterization of Wanninkof (1992). A weighted wind speed history approach was used to account for prior wind speed variability at the collection site (Reuer et al., 2007). The underlying assumption inherent in this calculation is that NCP has been constant over the mixed layer residence time (~ 10 days). Sporadic data gaps in the wind speed product means that we cannot calculate gas transfer velocities at all locations for which we have $\Delta O_2/Ar$ measurements. Lastly, entrainment or upwelling of O_2-undersaturated waters causes the biological O_2 flux to underestimate mixed layer NCP (Jonsson et al., 2013). This effect is strongest south of the PF where undersaturated Circumpolar Deep Water upwells and reaches the base of the mixed layer (Pollard et al., 2002). This study therefore focuses on the area between the STF and PF where the influence of this process is likely minimal.

Water column temperature profiles were collected along the transect at ~ 20 nautical mile intervals, using conductivity, temperature and depth (CTD) profiles, expendable bathythermographs (XBTs), and underway CTD (uCTD) casts. The research cruises used in this study are summarised in Table 1. In situ MLD was determined using the temperature difference criteria, $\Delta T = 0.2\,^{\circ}C$ in reference to the temperature at 10 m (De Boyer-Montégut et al., 2004). Summer MLD fields were also derived using the same temperature criteria from objectively analysed temperature profiles from the Hadley EN3 v.2a dataset (Ingleby and Huddleston, 2007). Monthly mean EN3 MLDs (MLD_{EN3}) are not ideal to assess shorter timescale variability, but it was preferable to use this data-based product instead of higher resolution modelled data sets. Accordingly, we only use MLD_{EN3} to represent the approximate magnitude and range of intraseasonal MLD variability in summer between 1998–2011 (i.e. the period best constrained by observations in the EN3 dataset). Photosynthetically Active Radiation (PAR) was taken from the standard monthly MODIS climatology product for summer months in units of mol photons $m^{-2}\,d^{-1}$ (http://oceancolor.gsfc.nasa.gov/cgi/l3) from 2002 to present.

BGD
11, 4335–4358, 2014

To assess short timescale in situ MLD variability, we used continuous water column temperature and salinity profiles of an autonomous glider deployed in the SAZ between September 2012 and February 2013 (described in Swart et al., 2014). Four hourly profiles were binned into 1 day bins to assess daily shoaling and deepening of the MLD. Deepening events along with mean iron profiles from the literature (Tagliabue et al., 2012) were used to calculate synoptic entrainment rates of dissolved iron from below the mixed layer.

3 Results

3.1 Meridional gradients and variability in MLD and $\Delta O_2/Ar$ ratios

Between 35° S–50° S, $\Delta O_2/Ar$ ratios tend to be low (0–2 %) when the MLD exceeds 45 m, but are generally elevated and highly variable (0–8 %) when the MLD is less than 45 m (Fig. 2a). A similar relationship of elevated and variable NCP is observed with shallow MLD, albeit with a reduced dataset (Fig. 2c). These results are consistent with earlier studies which show elevate primary production and NCP in shallow mixed layers, (e.g. Sakshaug and Holm-Hansen, (1986) (MLD < 40 m) and Cassar et al. (2011) (MLD < 50 m)) and support the canonical control of phytoplankton production by irradiance (Sverdrup, 1953). Geographically speaking, the high yet variable set of $\Delta O_2/Ar$ (and NCP) observations at MLDs shallower than 45 m are mainly confined to the mid-latitudes, between 38–46° S that encompass the SAZ (Fig. 2b and d).

Since mean PAR decreases and mean MLD_{EN3} increases consistently with increasing latitude from 35° S – 50° S (Fig. 3a and b), their latitudinal gradients alone cannot account for the observed mid-latitude (38–46° S) maxima and range in $\Delta O_2/Ar$ ratios (Fig. 2b and d). MLD_{EN3} meridional gradient (Fig. 3b) shows a strong contrast in the magnitudes and variability of MLDs with a rapid southward deepening of MLDs in the SAZ (40–45° S). In the STZ, MLD_{EN3} are shallow (average ~ 25 m) and characterised by low variability ($\sigma \pm 4.2$ m), whereas in the PFZ, MLD_{EN3} are deep and more variable

BGD
11, 4335–4358, 2014

(~ 70 ± 20.4 m). Only in the SAZ are MLD_{EN3} variable around the 45 m threshold where the maximum $\Delta O_2/Ar$ ratios are observed (Fig. 3b).

3.2 Intra-seasonal Fe supply and demand in the euphotic zone

Together with MLD driven light availability, NCP may also be responding to variations in the supply of iron that is driven by synoptic scale variations in mixing. Regional dFe concentration data (from the literature and summarised in Tagliabue et al., 2012) are limited to relatively few profiles (Chever et al., 2010; Klunder et al., 2011).

Daily synoptic mixed layer entrainment rates of dFe ($F_{Fe\text{-}syn}$ in units of nmol Fe m^{-2} d^{-1}) were estimated using a range of the number of positive daily MLD change events (i.e. deepening of MLD to below 45 m) taken from daily glider MLD data in the SAZ between September 2012 and February 2013 (Swart et al., 2014) and the available dFe profiles along the transect (data from Chever et al., 2010; Klunder et al., 2011).

$$F_{Fe\text{-}syn} = N/n \int_0^{MLD} \left(([dFe]_{subMLD} - [dFe]_{euphotic}) \times \frac{\Delta MLD_{45}}{MLD_t} \right) \cdot dz \quad (3)$$

Where $[dFe]_{subMLD}$ and $[dFe]_{euphotic}$ are the dFe concentrations from below the mixed layer and the euphotic zone respectively, MLD_t is the depth of the mixed layer after a daily deepening event, ΔMLD_{45} the difference between the observed MLD_t and a mixed layer of 45 m (the threshold identified for elevated NCP), and N is the number of events of entrainment over the month, and n the number of days in per month. In Eq. (3) the post entrainment concentration of dFe is scaled to the deepening of the MLD and the flux is derived by integration to the depth of the mean summer MLD. This correction for "detrainment" is important as this part of the entrained dFe is lost and no longer available to primary production when the MLD shoals following a deepening event. When mixed layers remained > 45 m for several consecutive days, the

BGD
11, 4335–4358, 2014

average MLD was used to calculate daily entrainment rates. To derive a mean daily dFe flux, all synoptic MLD deepening events to below 45 m were summed for each month and divided by the number of days per month. We assume that euphotic dFe concentration ranges between 0 nmol L^{-1}, reflecting complete consumption of dFe in the euphotic zone and 0.15 nmol L^{-1}, reflecting partial consumption of dFe concentrations, and a subsurface concentration of 0.25 nmol L^{-1}, taken from the profile data of Chever et al. (2010) and Klunder et al. (2011). Our overall goal was to test the sensitivity of the synoptic dFe entrainment flux to a weak and strong gradient in dFe, the extent of the MLD deepening and the number of events per month.

Glider data suggests the number of synoptic events would likely range between 2 and 5 per month and the mixed layer gradient perturbation would be between 1–35 m deeper than the 45 m threshold. Within this range, $F_{Fe\text{-}syn}$ is between 98–599 nmol Fe m^{-2} d^{-1}, depending on the surface and subsurface dFe concentrations, as well as the depth and frequency of the MLD deepening events (Fig. 5). Unsurprisingly, the largest $F_{Fe\text{-}syn}$ rates are found when the depth and frequency of deepening events in the glider data are the largest. In addition, $F_{Fe\text{-}syn}$ is enhanced markedly by assuming complete consumption of the euphotic zone dFe reservoir (compare Fig. 5b with 5a). Nevertheless, even the lowest rates of $F_{Fe\text{-}syn}$ estimated here (98 nmol Fe m^{-2} d^{-1}) are similar to or larger in magnitude than those associated with diapycnal diffusion (Boyd et al., 2005; Frants et al., 2013; Tagliabue et al., 2014).

4 Discussion

4.1 The role of MLD variability in driving NCP variability in the SAZ

Based on our observations of $\Delta O_2/Ar$ ratios, NCP and MLD, we consider a mechanism where intraseasonal synoptic scale MLD deepening entrains essential nutrients from below the euphotic zone, followed by rapid buoyancy driven shoaling of the MLD that creates favourable light conditions for phytoplankton growth. In the STZ, nutrient limita-

BGD
11, 4335–4358, 2014

tion through persistent shallow MLDs is known to limit primary production (Pollard et al., 2002; Joubert et al., 2011) preventing potentially high values of NCP. Here buoyancy forced stratification in the summer dominates over wind stress mixing (Swart et al., 2014). In the PFZ, wind stress mixing dominates over buoyancy forcing resulting in persistent deep MLDs, low mean PAR and low Fe concentrations (Chever et al., 2010; Klunder et al., 2011) that constrains NCP to a low range ($13.1 \pm 18\,\mathrm{mmol\,m^{-2}\,d^{-1}}$). The SAZ on the other hand lies between these two zonal modes and is characterised by a rapid meridional change in the mean MLD depth as well as MLD excursions above and below the critical 45 m light threshold for positive NCP (Figs. 3b and 4). These sub-seasonal MLD excursions around ~ 45 m are linked to a combination of intraseasonal high-wind-stress events (Swart et al., 2014) and restratification that is driven by mesoscale activity associated with fronts, mesoscale instabilities and eddies generated from interactions of the Antarctic Circumpolar Current (ACC) with topography and downstream advection (Swart and Speich, 2010).

It is possible that elevated and highly variable $\Delta O_2/Ar$ in the SAZ is due to MLD variability around a critical depth (~ 45 m) for NCP at intra-seasonal timescales. For example, in the North Atlantic, Mahadevan et al. (2012) showed that eddies increase water column stratification through eddy slumping when lateral (horizontal) density gradients destabilise the water column by transporting light water over dense water over weekly timescales. Such mechanisms rapidly reduce the depth of mixing leading to increased light exposure and more phytoplankton growth (Mahadevan et al., 2012). Similarly, Taylor and Ferrari (2011) showed that frontal instabilities can rapidly re-stratify the upper ocean (suppressing vertical mixing), even in the presence of strong surface cooling and destabilizing winds enhancing mean light exposure and triggering seasonal bloom development in low light conditions.

It is therefore feasible that intraseasonal high-wind-stress events characteristic of the SAZ (Braun, 2008; Swart et al., 2014) drive MLD deepening and nutrient entrainment, while increased buoyancy associated with high mesoscale activity creates the density gradients necessary to drive rapid re-stratification to < 45 m favouring mean light

BGD
11, 4335–4358, 2014

conditions for elevated production (Fig. 4). Repetition of this pattern on intraseasonal timescales reconciles both the observed highly variable NCP (0–80 mmolO_2 m^{-2} d^{-1}) in this study with sustained summer blooms characteristic of the SAZ (Thomalla et al., 2011; Swart et al., 2014). In this way, biomass can amass through production cycles driven by intra-seasonal re-supply of Fe (MLD > 45 m) and light (MLD < 45 m) at appropriate timescales for phytoplankton growth. This hypothesis however rests on the presence of both intraseasonal storm events deepening the mixed layer, which entrain limiting nutrients (primarily Fe) from below the euphotic zone, and subsequent stabilisation shallower than the critical NCP depth to alleviate light limitation that stimulates phytoplankton growth (depicted in Fig. 4).

4.2 Synoptic input of dissolved iron during summer

The role of synoptic inputs of iron to the euphotic zone in driving the variability of summer primary production has received little attention. Tagliabue et al. (2014) set out a seasonal paradigm of a large wintertime dFe pulse from entrainment followed by small addition of dFe supply from diapycnal diffusion that required high rates of dFe recycling to sustain summertime primary production. In this context, synoptic Fe fluxes can potentially provide a significant additional source of Fe. For example, the maximum summertime NCP we find is 80 mmol O_2 m^{-2} d^{-1}, which, assuming a photosynthetic quotient of 1.4 (Laws et al., 1991), is ~ 57 mmol C m^{-2} d^{-1}. This equates to an iron requirement of ~ 50 to 500 nmol Fe m^{-2} d^{-1} using Fe : C ratios typical of Southern Ocean phytoplankton (0.8–8.6 µmol Fe mol C^{-1}, Strzepek et al., 2011). The observational evidence however suggests that much of the phytoplankton iron demand is met by recycled iron (Bowie et al., 2009; Sarthou et al., 2008; Strzepek et al., 2005). Fe-ratio estimates range from 0.1 to 0.5 for low to high iron waters, which would imply a "new" iron requirement of ~ 5 to 250 nmol Fe m^{-2} d^{-1}. Overall, summertime dFe supply must therefore provide 5 to 500 nmol Fe m^{-2} d^{-1}, assuming a low to high reliance on "new" Fe input. Diapycnal fluxes from the Atlantic SAZ of 2–15 nmol Fe m^{-2} d^{-1} (Tagliabue et al., 2014) are clearly too low to support all but the lowest of our estimated Fe

BGD
11, 4335–4358, 2014

demand. In contrast, the synoptic dFe inputs of 100–600 nmol Fe m^{-2} d^{-1} more closely match demand estimates, suggesting that such supply mechanisms may be of importance in regions that experience strong variability in MLD dynamics over summer. In addition to the frequency and magnitude of the synoptic events themselves, the highest rates of synoptic dFe input require exhaustion of the surface dFe reservoir (Fig. 5). Unfortunately, currently available dFe observations in the Southern Ocean rarely constrain the seasonal minima in dFe (Tagliabue et al., 2012).

This additional flux of "new" dFe from synoptic events might also account for potential intraseasonal losses of dFe associated with detrainment when the mixed layer shoals following storm-driven deep mixing of phytoplankton biomass (Behrenfeld et al., 2013). This detrainment result in biomass export from the mixed layer and lost from the euphotic zone when organic matter is sequestered below the thermocline. Mixed layer deepening events can thus entrain new iron from a reservoir below the mixed layer on short timescales and replenish the Fe lost due to organic matter detrainment. Since this mechanism of entrainment/detrainment cycles has not been considered before, the implication is that low Fe-ratios potentially underestimate the contribution of new Fe in the iron budget.

The assumptions that underpin these calculated constraints to short-term event scale variability of productivity in the euphotic zone require a more vigorous test to assess synoptic entrainment fluxes. For instance, we found a strong sensitivity of synoptic input to the assumed surface dFe concentration which needs to be better constrained in the future (Tagliabue et al., 2012). In addition, our estimates of NCP were collected during the summer seasons of 2008–2010, dFe profiles were collected in summer 2008 (Chever et al., 2010; Klunder et al., 2011), and glider data were collected during summer 2012/13, and as such do not necessarily reflect the environmental conditions during the NCP observations. However, the iron and glider datasets were used to estimate the potential role of synoptic iron input rather than a precise value for a given year. Finally, top down processes (such as grazing) were not considered which may also influence phytoplankton biomass during deepening and shoaling of the mixed layer

BGD
11, 4335–4358, 2014

(Behrenfeld et al., 2013). In the future, a more comprehensive process study, similar to the FeCycle III experiment (Boyd et al., 2012), that accurately constrains Fe demand and its relation to mixed layer dynamics at the appropriate timescales is required.

5 In summary

In this study, we showed a strong non-linear relationship between NCP and MLD modulated by intraseasonal modes of variability in the Atlantic sector of the Southern Ocean, north of the Polar Front. The highest and most variable NCP were observed only when the MLD was < 45 m in the SAZ. The SAZ thus represents a dynamic transition zone between oligotrophic, shallow (< 45 m) and buoyancy-dominated stratified mixed layers to the north (STZ), and deep ($z > 45$ m) light-limited mixed layers to the south (PFZ). We propose that elevated and highly variable and sustained primary production in the SAZ results from intraseasonal scale storm events, alternating between deepening of the mixed layer, that entrains Fe, followed by rapid shoaling that favours growth in a transient iron replete, high light environment. We estimate rates of synoptic Fe fluxes to range between 100–600 nmol Fe m^{-2} d^{-1}, which are in the same order of magnitude as the Fe requirements for the observed elevated NCP. This dynamic helps explain the seasonal persistence primary production and biomass observed during summer in the SAZ (Swart et al., 2014). If this is correct, it highlights another potentially important climate sensitivity in respect of mid latitude ecosystems and the role of the SAZ in the biological carbon pump.

Acknowledgements. This study is part of the Southern Ocean Carbon and Climate Observatory (SOCCO) programme funded by CSIR Parliamentary Grant, ACCESS and NRF-SANAP programmes.We also like to thank Michael Bender for the $\Delta O_2/Ar$ and NCP data analysis at Princeton University.

BGD
11, 4335–4358, 2014

References

Arhan, M., Speich, S., Messager, C., Dencausse, G., Fine, R., and Boye, M.: Anticyclonic and cyclonic eddies of subtropical origin in the subantarctic zone south of Africa, J. Geophys. Res., 116, C11004, doi:10.1029/2011JC007140, 2011.

Arrigo, K. R., van Dijken, G. L., and Bushinsky, S.: Primary production in the Southern Ocean, 1997–2006, J. Geophys. Res., 113, C08004, doi:10.1029/2007JC004551, 2008.

Behrenfeld, M. J., Doney, S. C., Lima, I., Boss, E. S., and Siegel, D. A.: Annual cycles of ecological disturbance and recovery underlying the subarctic Atlantic spring plankton bloom, Global Biogeochem. Cy., 27, 526–540, doi:10.1002/gbc.20050, 2013.

Bowie, A. R., Lannuzel, D., Remenyi, T. A., Wagener, T., Lam, P. J., Boyd, P. W., and Trull, T. W.: Biogeochemical iron budgets of the Southern Ocean south of Australia: decoupling of iron and nutrient cycles in the subantarctic zone by the summertime supply, Global Biogeochem. Cy.,23(4), GB4034, doi:10.1029/2009GB003500, 2009.

Boyd, P. W.: Review of environmental factors controlling phytoplankton processes in the Southern Ocean 1, J. Phycol., 38, 844–861, 2002.

Boyd, P. W. and Ellwood, M. J.: The biogeochemical cycle of iron in the ocean, Nat. Geosci., 3, 675–682, doi:10.1038/ngeo964, 2010.

Boyd, P. W., Law, C. S., Hutchins, D. A., Abraham, E. R., Croot, P. L., Ellwood, M.,., Frew, R. D., Hadfield, M., Hall, J., Handy, S., Hare, C., Higgins, J., Hill, P., Hunter, K. A., LeBlanc, K., Maldonado, M. T., McKay, M., Mioni, C., Oliver, M., Pickmere, S., Pinkerton, M., Safi, K., Sander, S., Sanudo-Wilhelmy, A., Smith, M., Strzepek, R., Tovar-Sanchez, A., Wilhel, S. W., : Fe-cycle: attempting an iron biogeochemical budget from a mesoscale SF 6 tracer experiment in unperturbed low iron waters, Global Biogeochem. Cy., 19, GB4S20, doi:10.1029/2005GB002494, 2005.

Boyd, P. W., Jickells, T., Law, C. S., Blain, S., Boyle, E. A., Buesseler, K. O., Coale, K. H., Cullen, J. J., De Baar, H. J. W., Follows, M., Harvey, M., Lancelot., C., Levasseur, M., Owens, N. P. J., Pollard, R., Rivkin, R. B., Sarmiento, J., Schoemann, V., Smetacek, V., Takeda, S., Tsuda, A., Turner, S., Watson, A. J.,: Mesoscale iron enrichment experiments 1993–2005: synthesis and future directions, Science, 315, 612–617, doi:10.1126/science.1131669, 2007.

Braun, A. V.: A Comparison of Subtropical Storms in the South Atlantic Basin with Australian East-Coast Cyclones, American Meteorological Society, Conf. Proc., 2 B.5., 2008.

BGD
11, 4335–4358, 2014

Cassar, N., Barnett, B. A, Bender, M. L., Kaiser, J., Hamme, R. C., and Tilbrook, B.: Continuous high-frequency dissolved O_2/Ar measurements by equilibrator inlet mass spectrometry, Anal. Chem., 81, 1855–1864, doi:10.1021/ac802300u, 2009.

Cassar, N., DiFiore, P. J., Barnett, B. A., Bender, M. L., Bowie, A. R., Tilbrook, B., Petrou, K., Westwood, K. J., Wright, S. W., and Lefevre, D.: The influence of iron and light on net community production in the Subantarctic and Polar Frontal Zones, Biogeosciences, 8, 227–237, doi:10.5194/bg-8-227-2011, 2011.

Chever, F., Bucciarelli, E., Sarthou, G., Speich, S., Arhan, M., Penven, P., and Tagliabue, A.: Physical speciation of iron in the Atlantic sector of the Southern Ocean along a transect from the subtropical domain to the Weddell Sea Gyre, J. Geophys. Res., 115, C10059, doi:10.1029/2009JC005880, 2010.

Chisholm, S. W. and Morel, F. M. M.: What controls phytoplankton production in nutrient-rich areas of the open sea?, Limnol. Oceanogr., 36, U1507–U1511, 1991.

Craig, H. and Hayward, T.: Oxygen supersaturation in the ocean – biological vs. physical contributions, Science, 235, 199–202, 1987.

De Boyer Montégut, C.: Mixed layer depth over the global ocean: an examination of profile data and a profile-based climatology, J. Geophys. Res., 109, C12003, doi:10.1029/2004JC002378, 2004.

Falkowski, P. G., Laws, E. A., Barber, R. T. and Murray, J. W.: Phytoplankton, and their role in primary, new and export production, in: Ocean Biogeochemistry, edited by: Fasham, M. J. R., Springer, New York, 109–111, 2003.

Fauchereau, N., Tagliabue, A., Bopp, L., and Monteiro, P. M. S.: The response of phytoplankton biomass to transient mixing events in the Southern Ocean, Geophys. Res. Lett., 38,L17601, doi:10.1029/2011GL048498, 2011.

Frants, M., Gille, S. T., Hatta, M., Hiscock, W. T., Kahru, M., Measures, C. I., Mitchell, G. B., and Zhou, M.: Analysis of horizontal and vertical processes contributing to natural iron supply in the mixed layer in southern Drake Passage, Deep-Sea Res. Pt. II, 90, 68–76, doi:10.1016/j.dsr2.2012.06.001, 2013.

Ingleby, B. and Huddleston, M.: Quality control of ocean temperature and salinity profiles – historical and real-time data, J. Marine Syst., 65, 158–175, doi:10.1016/j.jmarsys.2005.11.019, 2007.

BGD
11, 4335–4358, 2014

Jonsson, B. F., Doney., S. C., Dunne, J., and Bender. M.: Evaluation of Southern Ocean O_2/Ar-based NCP estimates in a model framework, J. Geophys. Res., 118, 385–399, doi:10.1002/jgrg.20032, 2013.

Joubert, W. R., Thomalla, S. J., Waldron, H. N., Lucas, M. I., Boye, M., Le Moigne, F. A. C., Planchon, F., and Speich, S.: Nitrogen uptake by phytoplankton in the Atlantic sector of the Southern Ocean during late austral summer, Biogeosciences, 8, 2947–2959, doi:10.5194/bg-8-2947-2011, 2011.

Klunder, M. B., Laan, P., Middag, R., De Baar, H. J. W., and van Ooijen, J. C.: Dissolved iron in the Southern Ocean (Atlantic sector), Deep-Sea Res. Pt. II, 58, 2678–2694, doi:10.1016/j.dsr2.2010.10.042, 2011.

Lathuiliere, C., Levy, M., and Echevin, V.: Impact of eddy-driven vertical fluxes on phytoplankton abundance in the euphotic layer, J. Plankton Res., 33, 827–831, doi:10.1093/plankt/fbq131, 2010.

Laws, E. A.: Photosynthetic quotients, new production and net community production in the open ocean, Deep-Sea Res., 38, 143–167, 1991.

Lévy, M., Klein, P., and Ben Jelloul, M.: New production stimulated by high-frequency winds in a turbulent mesoscale eddy field, Geophys. Res. Lett., 36, L16603, doi:10.1029/2009GL039490, 2009.

Lévy, M., Ferrari, R., Franks, P. J. S., Martin, A. P., and Rivière, P.: Bringing physics to life at the submesoscale, Geophys. Res. Lett., 39, L14602, doi:10.1029/2012GL052756, 2012.

Mahadevan, A., D'Asaro, E., Lee, C., and Perry, M. J.: Eddy-driven stratification initiates North Atlantic spring phytoplankton blooms, Science, 337, 54–58, doi:10.1126/science.1218740, 2012.

Martin, H., Gordon, R. M., and Fitzwater, S. E.: Iron limitation?, The case for iron, Limnol. Oceanogr., 36, 1793–1802, 1991.

McGillicuddy, D. J., Anderson, L. A., Bates, N. R., Bibby, T., Buesseler, K. O., Carlson, C. A, and Steinberg, D. K.: Eddy/wind interactions stimulate extraordinary mid-ocean plankton blooms, Science, 316, 1021–1026, doi:10.1126/science.1136256, 2007.

Mitchell, B. G., Brody, E. A., Holm-Hansen, O., and Mcclain, C.: Light limitation of phytoplankton biomass and macronutrient utilization in the Southern Ocean Source, Limnol. Oceanogr., 36, 1662–1677, 1991.

Moore, J. K. and Abbott, M. R.: Phytoplankton chlorophyll distributions and primary production in the Southern Ocean, J. Geophys. Res., 105, 28709, doi:10.1029/1999JC000043, 2000.

BGD
11, 4335–4358, 2014

Oschlies, A. and Garcon, V.: Eddy-induced enhancement of primary production in a model of the North Atlantic Ocean, Nature, 398, 266–269, 1998.

Pollard, R. T., Lucas, M. I., and Read, J. F.: Physical controls on biogeochemical zonation in the Southern Ocean, Deep-Sea Res. Pt. II, 49, 3289–3305, 2002.

Sakshaug, E.L, and Holm-Hansen, O.: Photoadaptation in Antarctic phytoplankton: variations in growth rate, chemical composition and P vs. I curves, J. Plankton Res., 8, 459–473, 1986.

Reuer, M. K., Barnett, B. A., Bender, M. L., Falkowski, P. G., and Hendricks, M. B.: New estimates of Southern Ocean biological production rates from O_2/Ar ratios and the triple isotope composition of O_2, Deep-Sea Res. Pt. I, 54, 951–974, doi:10.1016/j.dsr.2007.02.007, 2007.

Sarthou, G., Vincent, D., Christaki, U., Obernosterer, I., Timmermans, K. R., and Brussaard, C. P. D.: The fate of biogenic iron during a phytoplankton bloom induced by natural fertilisation: impact of copepod grazing, Deep-Sea Res. Pt. II, 55, 734–751, doi:10.1016/j.dsr2.2007.12.033, 2008.

Siegel, D. A., Doney, S. C., and Yoder, J. A.: The North Atlantic spring phytoplankton bloom and Sverdrup's critical depth hypothesis, Science, 296, 730–733, doi:10.1126/science.1069174, 2002.

Strzepek, R. F., Maldonado, M. T., Higgins, J. L., Hall, J., Safi, K., Wilhelm, S. W., and Boyd, P. W.: Spinning the "Ferrous Wheel": the importance of the microbial community in an iron budget during the FeCycle experiment, Global Biogeochem. Cy., 19, GB4S26, doi:10.1029/2005GB002490, 2005.

Strzepek, R. F., Maldonado, M. T., Hunter, K. A., Frew, R. D., and Boyd, P. W.: Adaptive strategies by Southern Ocean phytoplankton to lessen iron limitation: uptake of organically complexed iron and reduced cellular iron requirements, Limnol. Oceanogr., 56, 1983–2002, doi:10.4319/lo.2011.56.6.1983, 2011.

Sverdrup, H. U.: On conditions for the vernal blooming of phytoplankton, J. Cons. Cons. Int. Explor. Mer., 18, 287–295, 1953.

Swart, S. and Speich, S.: An altimetry-based gravest empirical mode south of Africa: 2. Dynamic nature of the Antarctic Circumpolar Current fronts, J. Geophys. Res., 115, C03003, doi:10.1029/2009JC005300, 2010.

Swart, S., Speich, S., Ansorge, I. J., Goni, G. J., Gladyshev, S., and Lutjeharms, J. R. E.: Transport and variability of the Antarctic Circumpolar Current south of Africa, J. Geophys. Res., 113, C09014, doi:10.1029/2007JC004223, 2008.

BGD
11, 4335–4358, 2014

Swart, S., Thomalla, S. J., and Monteiro., P. M. S.: The seasonal cycle of mixed layer dynamics and phytoplankton biomass in the Sub-Antarctic Zone: a high resolution glider experiment, J. Marine Syst., 2014 (accepted manuscript).

Tagliabue, A., Mtshali, T., Aumont, O., Bowie, A. R., Klunder, M. B., Roychoudhury, A. N., and Swart, S.: A global compilation of dissolved iron measurements: focus on distributions and processes in the Southern Ocean, Biogeosciences, 9, 2333–2349, doi:10.5194/bg-9-2333-2012, 2012.

Tagliabue, A., Sallée, J- B., Bowie, A. R., Lévy, M., Swart, S., and Boyd, P. W.: Surface water iron supplies in the Southern Ocean sustained by deep winter mixing, Nat. Geosci., doi:10.1038/ngeo2101, (accepted manuscript), 2014.

Taylor, J. R. and Ferrari, R.: Ocean fronts trigger high latitude phytoplankton blooms, Geophys. Res. Lett., 38, L23601, doi:10.1029/2011GL049312, 2011.

Thomalla, S. J., Fauchereau, N., Swart, S., and Monteiro, P. M. S.: Regional scale characteristics of the seasonal cycle of chlorophyll in the Southern Ocean, Biogeosciences, 8, 2849–2866, doi:10.5194/bg-8-2849-2011, 2011.

Wanninkhof, R.: Relationship between wind speed and gas exchange over the ocean, J. Geophys. Res., 97, 7373–7383, 1992.

BGD
11, 4335–4358, 2014

Table 1. List of research cruises during summers of 2008–2010 and relevant parameters during this study.

Program	Cruise type	Research Vessel	Date	Parameters
Bonus GoodHope	IPY process study	RV Marion Dufresne	13 Feb 2008–17 Mar 2008	$\Delta O_2/Ar$, CTD, XBT
SANAE 48 Leg1	Underway	MV SA Agulhas	23 Dec 2008–4 Jan 2009	$\Delta O_2/Ar$, uCTD, XBT
SANAE 48 Leg6	Underway	MV SA Agulhas	21 Feb 2009–5 Mar 2009	$\Delta O_2/Ar$, uCTD, XBT
SANAE 49 Leg1	Underway	MV SA Agulhas	9 Dec 2009–22 Dec 2009	$\Delta O_2/Ar$, uCTD, XBT
SANAE 49 Leg6	Underway	MV SA Agulhas	13 Feb 2010–23 Feb 2010	$\Delta O_2/Ar$, uCTD, XBT

uCTD – underway Conductivity, Temperature, Depth profiles.
XBT – expendable bathythermograph profiles.
Underway measurements were conducted on a ship of opportunity (MV SA Agulhas) during the summer logistics voyages to Antarctica.

BGD
11, 4335–4358, 2014

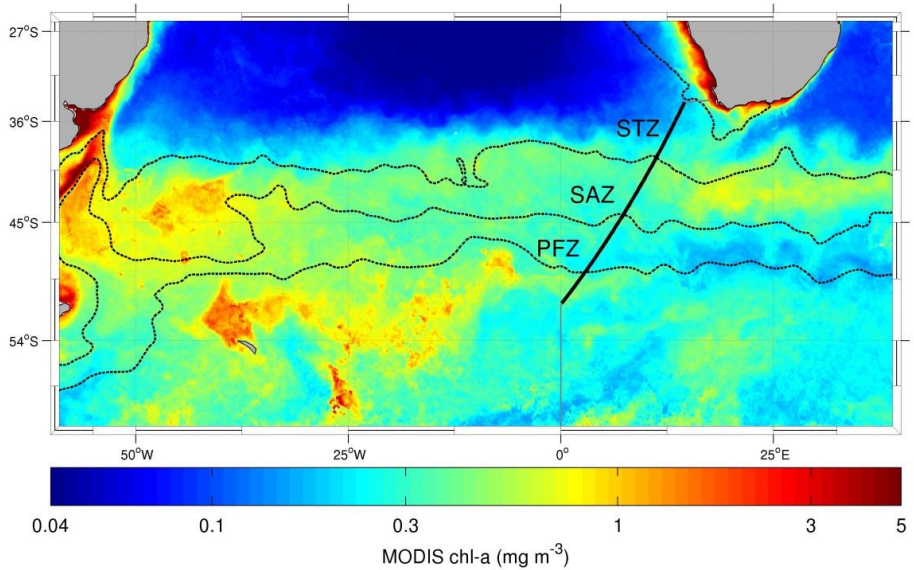

Fig. 1. Sampling track overlaid on the summer climatology for MODIS satellite observed chl *a* showing the zonally constrained elevated chl *a* concentrations in the Sub-Antarctic Zone. Also depicted are the Subtropical Zone (STZ), SubAntarctic Zone (SAZ) and the Polar Frontal Zone (PFZ) delineated by the Sub-tropical front (STF), Sub-Antarctic Front (SAF), and Polar Front (PF). Frontal positions (black dotted lines) are calculated from mean absolute dynamic topography.

BGD
11, 4335–4358, 2014

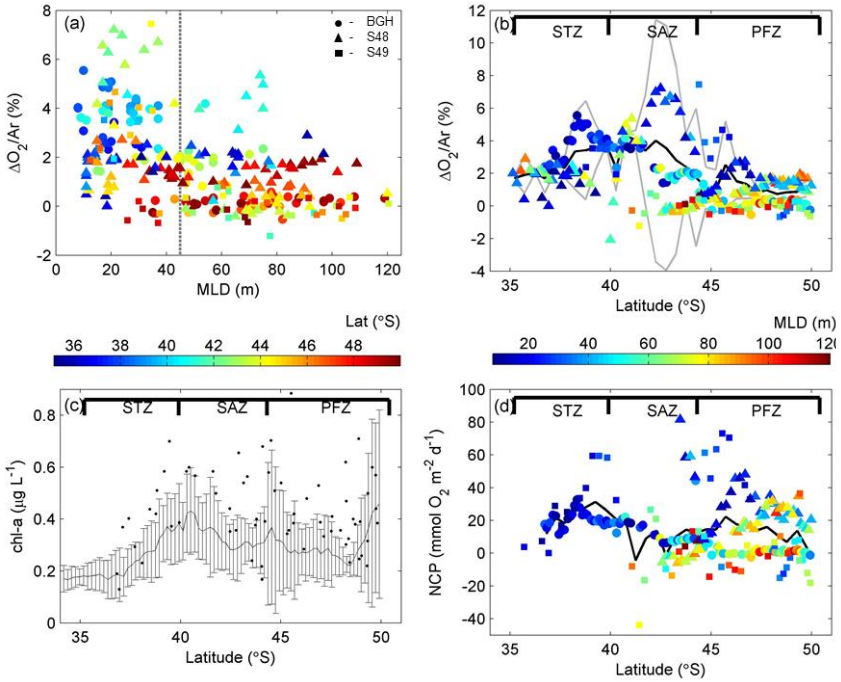

Fig. 2. (a) Relationship of $\Delta O_2/Ar$ ratios with MLD shows two modes of variability: deep mixed layers (> 45 m) show diminished biological supersaturation, while shallow mixed layers (< 45 m) increased biological supersaturation with high variability. Colorbar indicates the latitude while circles, triangles and squares represent the three summer cruises, namely Bonus-Good Hope (BGH), SANAE48 (S48) and SANAE49 (S49) respectively. **(b)** Latitudinal $\Delta O_2/Ar$ ratios (%) show the highest variance (grey lines) in the Sub-Antarctic Zone between 38–46° S. Variance is calculated from $\Delta O_2/Ar$ data binned in 0.5° latitude bands. The colorbar for **(b)** and **(d)** indicates the corresponding MLD. The mean locations of the frontal zones, as determined using the mean absolute dynamic topography are displayed at the top for all latitudinal figures. **(c)** NCP vs. MLD. **(d)** Latitudinal NCP calculated using Eq. (2).

BGD
11, 4335–4358, 2014

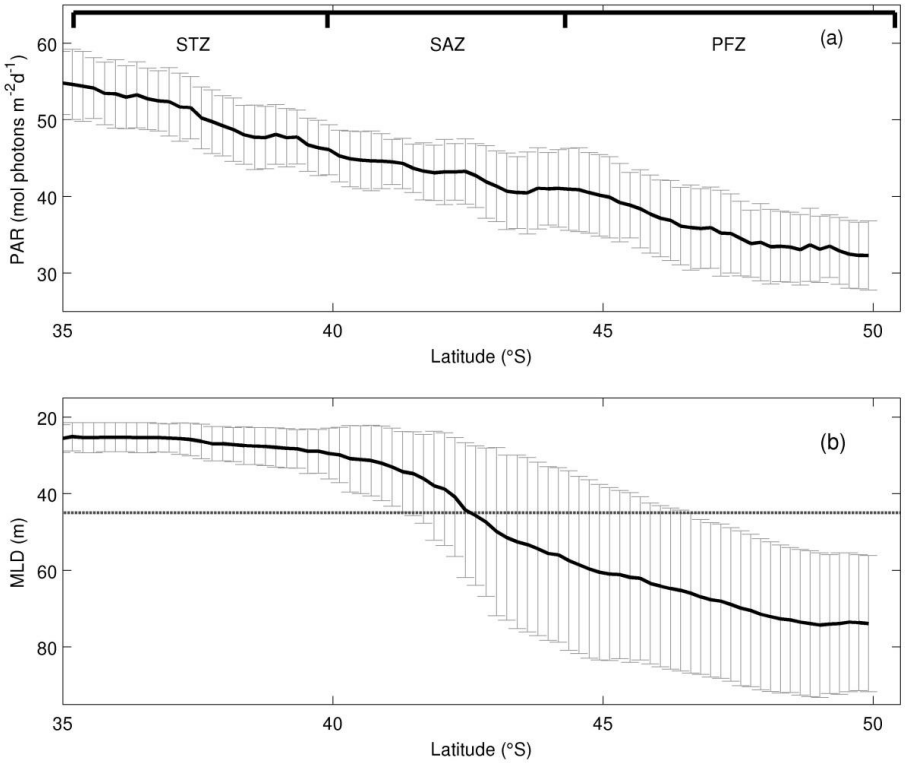

Fig. 3. (a) MODIS surface Photosynthetically Active Radiation climatology for summer months (DJF) in units of mol photons $m^{-2} d^{-1}$ along the cruise track from 2002 to present. **(b)** Summer climatological MLD and associated standard deviation, shows a steep gradient in the SAZ which separates the shallow, low variability MLD to the north and the deep, highly variable MLD to the south.

BGD
11, 4335–4358, 2014

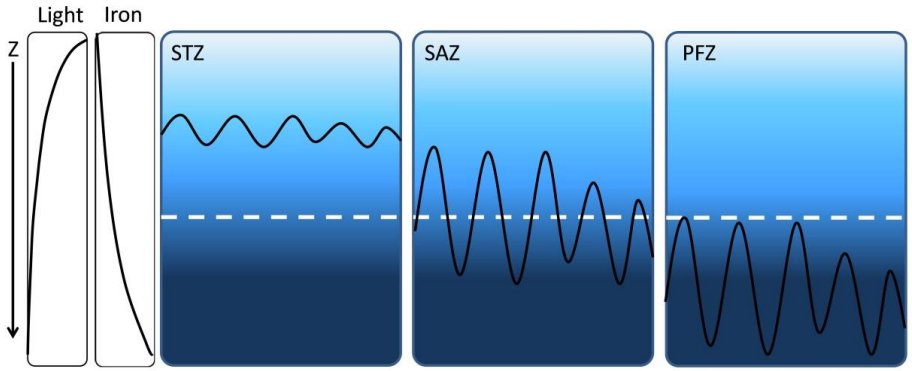

Fig. 4. Conceptual model shows MLD variability (black line) in the STZ, SAZ and PFZ, in relation to a water column irradiance depth threshold (dotted white line). This model proposes that the SAZ is the only region where the MLD deepening, driven by short term storm events, followed by shoaling during quiescent periods drives short term variability in phytoplankton production.

BGD
11, 4335–4358, 2014

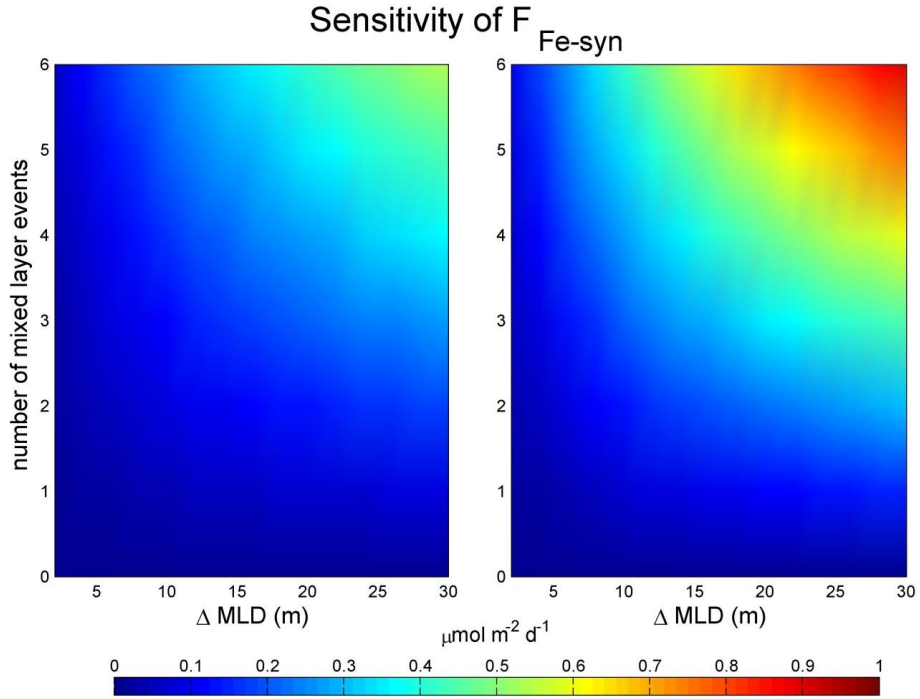

Fig. 5. Sensitivity of synoptic dFe flux rates to number of deepening events and change in the MLD. The left and right panels represent a surface dFe concentration of 0.15 nM (conservative estimate) and 0 nM (assuming complete surface consumption of iron) respectively.

BGD
11, 4335–4358, 2014